Available online at www.sciencedirect.com
SCIENCE DIRECT®
Solar Energy Materials & Solar Cells
ELSEVIER
Solar Energy Materials & Solar Cells 90 (2006) 2099–2106
www.elsevier.com/locate/solmat

Purification of metallurgical grade silicon by a solar process

G. Flamant[a,*], V. Kurtcuoglu[b], J. Murray[a], A. Steinfeld[b,c]

[a]*Processes, Materials and Solar Energy Laboratory (PROMES)-CNRS, 7 rue du four solaire, Odeillo, 66120 Font Romeu, France*[1]

[b]*Department of Mechanical and Process Engineering, ETH-Swiss Federal Institute of Technology Zurich, 8092 Zurich, Switzerland*[1]

[c]*Solar Technology Laboratory, Paul Scherrer Institute, 5232 Villigen, Switzerland*

Received 20 October 2005; accepted 9 February 2006
Available online 4 April 2006

Abstract

The purification of upgraded metallurgical silicon by extraction of boron and phosphorus was experimentally demonstrated using concentrated solar radiation in the temperature range 1550–1700 °C. The process operated with a flow of Ar at reduced pressure (0.05 atm) for elimination of P, and with a flow of H_2O for elimination of B. Impurity content decreased by a factor of 3 after a 50-min solar treatment, yielding Si samples with final average content of 2.1 ppm_w B and 3.2 ppm_w P.

Keywords: Solar chemistry; PV silicon; Purification of silicon; Silicon metallurgy; Solar thermal process

0. Introduction

The worldwide solar cell production reached 1256 MW_p in 2004, a 67% increase over the 2003 output [1]. Crystalline silicon solar cells, particularly multi-crystalline silicon, made up of more than 90% of the world PV production [2]. Most of the solar grade silicon (SGS) used for PV applications stems from rejects of electronic grade silicon (EGS) used in the electronic industry. However, its annual supply is surpassed by its demand, urging the

*Corresponding author. Tel.: +33 468 307758; fax: +33 468 302940.
E-mail address: flamant@promes.cnrs.fr (G. Flamant).

[1]PROMES and ETHZ are Members of "SolLab" (Alliance of European Laboratories for Research and Technology on Solar Concentrating Systems).

0927-0248/$ - see front matter
doi:10.1016/j.solmat.2006.02.009

need for novel technological solutions for the processing of SGS at a target price of 12–15 €/kg and target demand of 10 g/W_p [3,4]. Similarly to EGS production, the route for SGS processing uses metallurgical grade silicon (MGS) as starting material. Annual world production of MGS amounts to 1 million tons, obtained by quartz reduction in arc furnaces. The process reaction is

$$SiO_2 + 2C \rightarrow Si + CO, \quad \Delta H_{298\,K} = 695\,kJ. \tag{1}$$

The production of 1 ton of MGS requires 2.9–3.1 ton quartz, 1.2–1.4 ton coke, 1.7–2.5 ton charcoal, 0.12–0.14 ton graphite (electrodes), and 12.5–14 MWh electricity [5]. The purity varies from 98.5% up to 99.5%, and the average price is 1.5–2.5 €/kg, depending on quality [3]. Some of the typical impurities are Fe, Al, Ca, Ti, Cr, B, P, O, and C. The production of EGS from MGS requires a reduction of these impurities by at least five orders of magnitude. Consequently, EGS processing occurs via distillation of silicon gaseous compounds at 35–50 €/kg. Purification of MGS is an optional chemical path among the routes for processing SGS. Other routes include reaction of silicon dioxide and carbon with high purity and silicon halogenide reduction with high-purity reduction materials. Purification can be accomplished using plasma techniques [6,7]. In particular, an inductive plasma torch combined with an inductive cold crucible in a chamber was used to treat 30 kg of upgraded metallurgical silicon (UMGS) per batch. PV cells processed with the resulting material exhibited a conversion efficiency of 12.4% [7], compared with 10.12% measured on the starting material [8]. Boron removal is considered to be critical due to its rather high segregation coefficient that prevents its removal by controlled solidification. Plasma treatment with steam and directional solidification steps allowed the removal of B and other metallic impurities [9]. The main drawback of the plasma purification process is its high electricity consumption that governs the process cost (21 €/kg in 2002, without manpower [7]). Alternatively, concentrated solar energy can replace the plasma torch and be used as the source of high-temperature process heat. In contrast to a plasma-driven process, no excited species are formed at the reaction surface in the solar-driven process. This paper examines the solar purification of MGS, aimed at the removal of boron and phosphorus by vaporisation. Thermodynamic equilibrium computations are carried out for determining temperature and pressure requirements and product gas compositions. The experimental set-up and main experimental results are presented and discussed.

1. Thermodynamics

Thermodynamic equilibrium computations were carried out using HSC code [10]. For most calculations, the silicon feed was assumed to consist of 1 kmol silicon, 0.05 mol water, 10 ppm_w phosphorus, and 6 ppm_w boron mixed with a large excess of argon (100 kmol) in order to account for the renewing of the buffer gas during the experiments. Other impurities accounted were: 300 ppm_w Ca, 100 ppm_w Mn and Ni; 50 ppm_w Fe and Al, 10 ppm_w Cr and C; and 5 ppm_w Ti. These concentrations correspond to levels that may occur in UMGS, see Table 1.

The chemical species existing at equilibrium for the Si–O–H–Ar system are shown in Fig. 1 (argon is not included in the plot). SiO and Si vapors are formed at 1200–1700 °C, respectively. Therefore, this later temperature may be considered as the upper limit of operating temperature to prevent any significant silicon vaporisation.

Table 1
Impurity concentrations in UMGS (target, from Ref. [4]), in RIMA Si and in SGS (target, from Ref. [4]). All values in ppm_w

Impurities	UMGS	RIMA Si	SGS
B	<30	5.7	<1
P	<15	9.4	<5
O	<2000	–	<10
C	<250	–	<10
Fe	<150	35	<10
Al	<50	57	<2
Ca	<500	320	<2
Ti	<5	2.6	<1
Cr	<15	–	<1

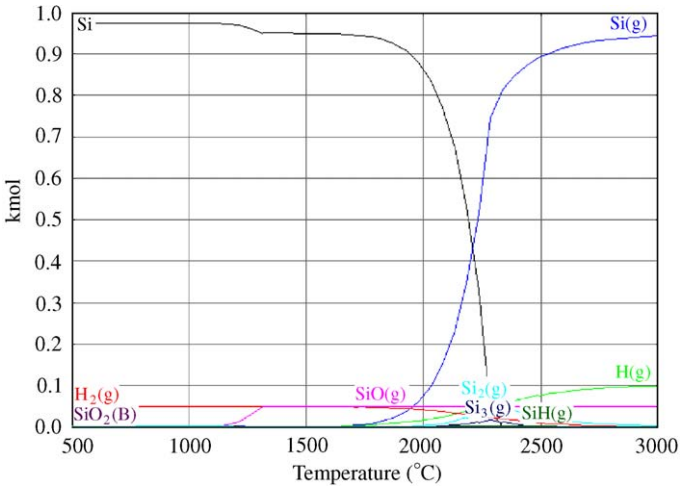

Fig. 1. Chemical equilibrium composition for 1 kmol Si, 0.05 kmol H_2O and 100 kmol argon at 1 atm.

According to Ref. [7], boron can be extracted in the gaseous form as BOH, BO, BH_2 and B_2O_2 but the vapor pressure of BOH is at least one order of magnitude larger than that of the other species in the temperature range 1500–1700 °C. HSC software considers only BOH (because of the lack of thermodynamic data concerning the other species) that is formed even at low temperature, as shown in Fig. 2. The same figure indicates that the phosphorus extraction, in the elementary form P or P_n ($n = 2$, 3 or 4), requires temperatures higher than 1500 °C (in Fig. 2, P, P(B) and P(R), indicate white, black and red phosphorus, respectively). A pressure reduction favours the phosphorus elimination but it does not affect the boron behaviour.

The influence of other impurities on B and P extraction was also studied; main impurities such as Ca, Mn, Ni, Fe, Al, Cr, C and Ti were taken into account. The results are not illustrated here due to the large number of chemical species (more than 30) existing at equilibrium. No formation of any new boron species is predicted. Phophorus can form binary compounds with Si (Si_2P, SiP) and phosphates such as $Ca_4(PO_4)_2(OH)$, which have

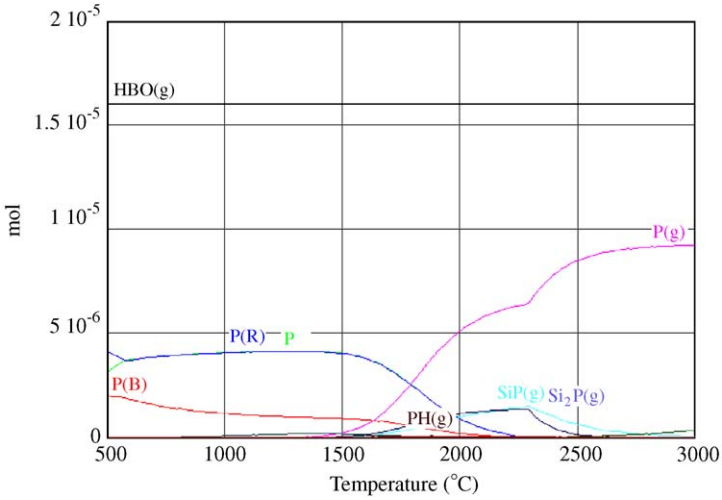

Fig. 2. Chemical equilibrium composition for 1 kmol Si, 0.05 kmol H_2O, 10 ppm_w P and 6 ppm_w B in argon (100 kmol) at 1 atm.

a negligible influence on P vaporisation. For the rest of elements, many Si-based binary alloys exist in the temperature range 1500–1700 °C, for example, FeSi, $FeSi_2$, Mn_xSi_y, $TiSi_2$, $CrSi_2$, etc. Silicates of Ca, Fe and Al are also stable.

As a conclusion of this thermodynamic study, the favourable temperature range for Si purification (removal of B and P) is about 1500–1700 °C. Temperatures above 1500 °C are needed in order to reach a significant P vapor pressure.

2. Experimental set-up

The experimental set-up is depicted in Fig. 3. The vertical-axis solar furnace of the PROMES Laboratory (Odeillo) consists of a sun-tracking flat heliostat on axis with a 2 m-diameter parabolic concentrator (Fig. 3a), capable of delivering peak solar concentration ratios of 16 000 and attaining temperatures up to 3200 °C. The reactor was placed at its focus. Concentrated solar radiation entered the reactor through a Pyrex window and heated the sample (typically 3 g) placed on a water-cooled crucible. Rapid heating or cooling of the sample (about 10 ms) was controlled by a radiation shutter. Gas ports were used for controlling the operating pressure and for injecting buffer gas (Ar) and reacting gas (H_2O). Before each experimental run, the reactor was filled with Ar and evacuated two times. The measurement system included pressure gauge, gas flow meters, pyrometers, and direct solar irradiation (DNI) data. A 1.39 μm solar-blind pyrometer was employed for measuring the surface temperature of a sample of known emissivity [11] (this apparatus is named "main pyrometer" in Fig. 4). A second 0.65 μm pyrometer was employed as a detector for controlling the opening/closing of the shutter (this apparatus is named "fast pyrometer" in Fig. 4). Injection of H_2O was performed using two systems: a ex situ humidifier based on a saturated Ar flow through a heated water bath, and a in situ humidifier based on water vaporisation on hot surface inside the reactor. The former device allowed control of amount of water injected, while no control was possible with the

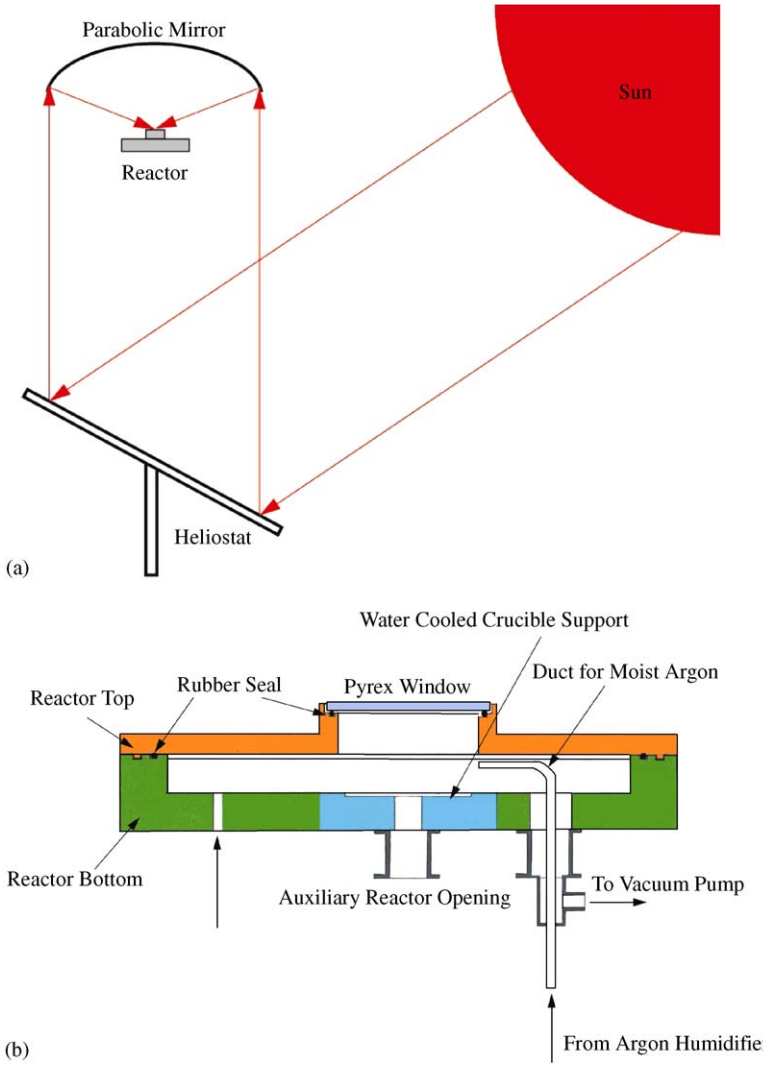

Fig. 3. Solar experimental set-up: (a) principle of the solar furnace and (b) scheme of the solar reactor.

latter one. The starting material was UMGS provided by RIMA [12]. The typical composition of the UMGS and the required composition of SGS are listed in Table 1. The mean B and P concentrations in the Si feedstock must be reduced by about five and two times, respectively, to reach the SGS specifications. Analysis of B and P contents was performed by ICP-OES [13]. The sample was crushed before sampling for analysis consequently the results correspond to mean concentration of B and P.

3. Experimental results

Experiments have been carried out at 0.05 atm to favour P vaporisation, using 1 l/min Ar + 2.5 ml H_2O to favours B vaporisation as BOH, and in the temperature range

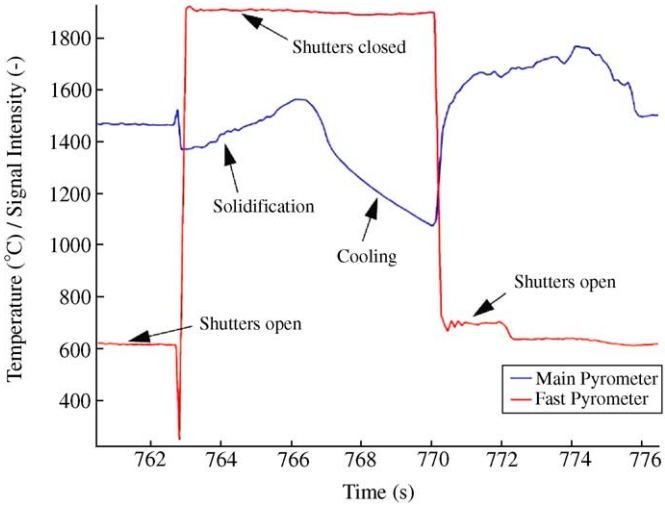

Fig. 4. Variation of measured sample temperature during shutter closing in a representative solar experimental run.

1550–1700 °C to favour P evaporation but may result in SiO formation. Fig. 4 shows an example of temperature monitoring during a representative solar run. The measured signal was not corrected for the samples' emissivity, which can vary between 0.7 for Si(s) and 0.1–0.3 for Si(l), and is affected by impurities [14]. At about $t = 763$ s the shutter was closed. The sample temperature showed a slight increase at the very beginning of the cooling process. This phenomenon was a perturbation due to the shutter movement. Then a small decrease of the temperature signal was due to shadowing. A temperature increase was measured during the solidification process as a result of an increase in the sample's emissivity. At the end of solidification ($t = 766$ s) the measured temperature (Fig. 4) was about 1500 °C, above the silicon m.p. 1414 °C. This difference may be due either to surface composition of the sample (not pure Si) or to parasitic radiation coming from the reflected solar beam.

Sample composition as a function of treatment time (10, 30 and 50 min) is illustrated in Fig. 5, and listed in detail in Table 2. Initial B and P contents were 5.7 and 9.4 ppm_w, respectively. Runs 2–5 verified the reproducibility of the experiments. After 50 min, the B and P contents in the sample were 2.1 and 3.2 ppm_w, respectively, which correspond to 270% and 294% decrease of B and P, respectively. Run 1 indicates a slight increase of B and P content in the sample, as a result of measurement uncertainty [11]. No significant purification was observed after 10 min. For the 30-min runs, the final B concentration was in the range 2.8–4.4 ppm_w, with a mean value of 3.85 ppm_w; the final P concentration was in the range 2.4–6.2 ppm_w, with a mean value of 4.55 ppm_w. Table 3 further shows that B is not eliminated by using pure Ar, whereas P content decreases significantly after 40 min of solar treatment in pure Ar at reduced pressure.

Measurement uncertainty, variation of sample initial composition, and variation of temperature during solar processing contribute to the data dispersion. According to SCA [13], the measurement uncertainty of B and P content in the samples is $\pm 10\%$. Analysis of B and P concentration in the feedstock indicates a $\pm 15\%$ variation of sample initial

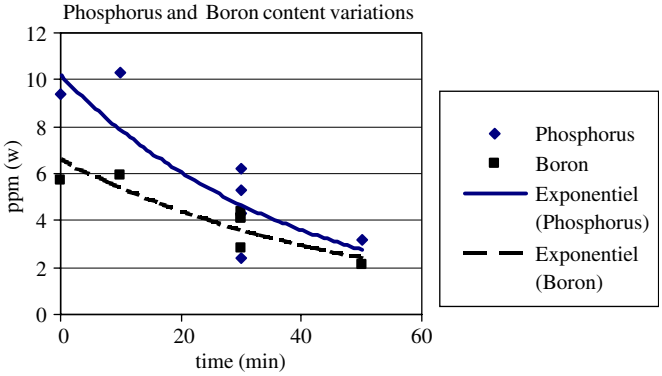

Fig. 5. Variation of boron and phosphorus contents as a function of treatment time (see Table 2). Pressure: 0.05 atm, argon: 1 l/min, water: 2.5 ml.

Table 2
Boron and phosphorus sample composition as a function of treatment time for solar experimental runs with H_2O–Ar (pressure: 0.05 atm, argon: 1 l/min, water 2.5 ml). All values in ppm_w

Run	0	1	2	3	4	5	6
Time (min)	0	10	30	30	30	30	50
P	9.4±2.4	10.3±2.5	5.3±1.3	2.4±0.6	6.2±1.5	4.3±1.1	3.2±0.8
B	5.7±1.4	5.9±1.5	4.4±1.1	4.1±1	2.8±0.7	4.1±1	2.1±0.5

Table 3
Boron and phosphorus sample composition for solar treatment in pure Ar

Run	0	7	8
Pressure (atm)	–	0.085	0.05
Argon flow rate (l/min)	–	2.5	1
Time (min)	0	40	60
P (ppm_w)	9.4±2.4	6±1.5	5.5±1.4
B (ppm_w)	5.7±1.4	4.8±1.2	6.4±1.6

composition. Assuming an overall ±25% uncertainty, the experimental data show an efficient removal of B and P from Si after 50-min solar processing. Further, experimental results are consistent with the thermodynamic predictions. Boron elimination requires H_2O as reacting gas. Phosphorus can be extracted in pure Ar and low pressure. Formation of SiO_2 inside the reactor was observed in the cold internal wall, as a result of SiO(g) oxidation.

A solar process for UMGS purification may be designed on the basis of two reactor concepts: a rotary kiln reactor and a molten bath reactor. The rotary kiln reactor, which features a self-crucible of same solid material containing the liquid phase was successfully used to process refractory oxides [15]. Since the depth of the liquid is generally small

(10–20 cm), no additional stirring is necessary. The molten bath reactor concept was successfully tested for Zn production by carbothermic reduction of ZnO using a beam down solar concentrating system [16,17]. Electromagnetic stirring of the molten material should be maintained for this reactor concept.

4. Conclusion

We have performed thermodynamic equilibrium calculations to determine the gas composition over UMGS in argon over a wide temperature range. Boron may be extracted mainly as BOH(g) at low temperatures when steam is added; phosphorus may be extracted as gaseous P above 1500 °C and 1 bar. Pressure reduction further favours P elimination. We have carried out set of solar experimental runs in a solar furnace with batch samples of UMGS. The process operated at reduced pressure (0.05 atm) for elimination of P, and with H_2O (humidified argon) for elimination of B. Concentrations of phosphorus and boron in the samples were reduced by a factor of about 3 after 50-min of solar irradiation in the 1550–1700 °C range. Replacing a plasma-driven process by concentrated solar radiation eliminates electricity consumption and further avoids the contamination of the reaction chamber with ionised species.

Acknowledgements

Authors acknowledge RIMA for providing UMGS, Ch. Trassy (EPM Lab, Grenoble, France) for fruitful discussion; and D. Gauthier and A. Ferriere (PROMES-CNRS) for assistance during material analysis and experiments.

References

[1] M. Schmela, PHOTON International, March 2005.
[2] T. Surek, J. Crystal Growth 275 (2005) 292.
[3] P. Woditsch, W. Koch, Sol. Energy Mater. Sol. Cells 72 (2002) 11.
[4] D. Sarti, R. Einhaus, Sol. Energy Mater. Sol. Cells 72 (2002) 27.
[5] W. Zulehner, "Silicon"; Ullmann's Encyclopedia of Industrial Chemistry, vol. A23, 1993.
[6] D. Morvan, I. Cazard-Juvenat, J. Amouroux, J. Mater. Res. 13 (1998) 270.
[7] C. Alemany, C. Trassy, B. Pateyron, K.-I. Li, Y. Delannoy, Sol. Energy Mater. Sol. Cells 72 (2002) 41.
[8] S. De Wolf, J. Szlufcik, Y. Delannoy, I. Périchaud, C. Hässler, R. Einhaus, Sol. Energy Mater. Sol. Cells 72 (2002) 49.
[9] N. Huge, H. Baba, Y. Sakaguchi, K. Nishikawa, H. Terashima, F. Aratami, Sol. Energy Mater. Sol. Cells 34 (1994) 243.
[10] HSC Chemistry, Outokumpu Research Oy, Pori, Finland, 2002.
[11] D. Hernandez, G. Olalde, J.M. Gineste, C. Geymard, ASME J. Sol. Energy Eng. 126 (2004) 645.
[12] ⟨http://www.rima.com.br⟩.
[13] Service Central d'Analyse du CNRS, Echangeur de Solaize, BP 22, 69390 VERNAISON, France. ⟨http://www.sca.cnrs.fr⟩.
[14] A. Yeckel, A.G. Salinger, J.J. Derby, J. Cryst. Growth 152 (1995) 51.
[15] C. Royere, Entropie 97 (1881) 147.
[16] E. Guillot, M. Epstein, C. Wieckert, G. Olalde, A. Steinfeld, S. Santén, U. Frommherz, S. Kräupl, T. Osinga, ISEC 2005, August 6–12, 2005, Orlando, FL, USA.
[17] A. Yogev, A. Kribus, M. Epstein, A. Kogan, Int. J. Hydrogen Energy 23 (1998) 245.